Eye Tracking Calibration based on Smooth Pursuit with Regulated Visual Guidance

Yangyang Li[1,2][a], Lili Guo[1][b], Guangbin Sun[1,*][c], Rongrong Fu[3][d], Zhen Yan[1][e] and Ji Liang[1][f]

[1]*Technological and Engineering Center for Space Utilization of Chinese Academy of Sciences,*
No. 9 Deng Zhuang South Rd., Beijing, 100094, China
[2]*University of Chinese Academy of Sciences, No. 19(A) Yuquan Rd., Beijing, 100049, China*
[3]*Yanshan University, No. 438 West Hebei Avenue, Qinhuangdao, Hebei, 066004, China*

Keywords: Eye Tracking, Smooth Pursuit, Gaze Calibration, Visual Guidance, Neural Network.

Abstract: Eye tracking calibration based on smooth pursuit has the characteristics of rapidity and convenience, but most smooth pursuit calibration methods are based on spontaneous and passive gazes. The spatial-temporal characteristics of the target movement can significantly affect the tracking performance, but few works have performed calibration considering the effects of both the spatial and temporal variance of the smooth pursuit target. Therefore, we proposed an off-line smoothing pursuit calibration featuring actively regulated speed under specially designed visual guidance paths. In our prelude experiments, we found that there was an obvious correlation between the eye movement velocity and the error of gaze point measurement. In particular, when the movement velocity of gaze exceeded 6°/s, the accuracy and precision of the eye-tracking system were obviously lower. Based on these findings, the visual guidance trajectory was regulated, with the speed kept below 6°/s. The smooth pursuit calibration was combined with the neural network learning method. The results showed that the mean absolute error was reduced from 1.0° to 0.4°, and the full calibration process took only approximately 45 seconds.

1 INTRODUCTION

Human eye gaze behaviour has the dual function of information acquisition and signal transmission (Valtakari et al., 2021). Eye tracking is a sensor measurement technology that is generally used in human-computer interaction. Analysing the eye movement of users through eye tracking is helpful for understanding some of the user's intentions (Hansen, Ji, & intelligence, 2009). Humans usually prefer the human-computer interaction mechanism with a functionally intuitive interface and simple setting procedures for ease and productiveness, while the complex and incomprehensible human-computer interaction mechanism will impose a burden on users due to poor usability. From this perspective, the interaction of eye movement tracking is qualified with intuitive and simple interaction characteristics.

Eye tracking systems can be divided into two types: invasive and noninvasive trackers. Most tracking systems in practice are noninvasive based on optical principles. Noninvasive eye tracking systems can be divided into desktop and head-mounted counterparts in practice (Mahmud, Lin, & Kim, 2020). Desktop eye tracking systems are based on proximal fixed monitors and interact with digital information from sensor streams and/or actionable intelligent agents. They can work far away from the target object, such as SMI RED250, Tobii Eye Tracker5, Kinect and so on. This kind of equipment contains a user-oriented camera, which is used to capture the user's facial image. According to the

[a] https://orcid.org/0000-0002-5769-7596
[b] https://orcid.org/0000-0002-4390-2640
[c] https://orcid.org/0000-0002-2939-2066
[d] https://orcid.org/0000-0003-0350-7619
[e] https://orcid.org/0000-0003-2757-1623
[f] https://orcid.org/0000-0001-9068-7990

extracted features from the facial image, the gaze point on the screen can be calculated. Head-mounted eye tracking systems, such as SMI Glasses and Tobii Pro Glasses3, contain at least two eye cameras to capture eye images directly, in addition to the user-faced camera with a scene camera to capture the scene image, and estimate the user fixation points through the eye images and the scene image. Head-mounted equipment is more flexible, but it has a compact design for portability; therefore, the performance of hardware such as cameras and computing elements is low, with poor data sampling and processing ability. In addition, the head-mounted device has two other limitations: eccentric eye movement (the eye tracking camera of the head-mounted device has difficulty capturing eye movement close to the edge) and coordinate system variation (when tracking the target object in the real scene, the position of the target object will change with the user's head position and user movement, and there is a large difference in the data representation of the same target tracking between users).

For remote and noninvasive eye tracking systems, the commonly used technology is Pupil Center-Corneal Reflection technology (PCCR) (Larrazabal, Cena, Martínez, & medicine, 2019; Zhu & Ji, 2005). Near-infrared light is used to generate a reflective flash on the surface of the cornea, and then the reflection image is captured by the camera. The reflection of the light source is identified by the reflection image in the cornea and pupil, and a vector between the cornea and pupil is established, which is called the fixation vector. Based on the mapping model, the gaze position is calculated.

To establish the mapping model, parameters (Guestrin & Eizenman, 2006), such as the pupil center, corneal curvature center, optical axis and visual axis, need to be acquired. The parameters of the eyeball model are subject dependent, so user calibration is needed before the normal use of an eye tracking system to collect data of parameters with individual differences; meanwhile, the process and method of calibration greatly affect the quality of eye tracking data (Holmqvist et al., 2011). In addition, with the passage of time, the estimation of the gaze point by the mapping model of the eye tracking system will become inaccurate for parameter drifting. This will happen when the system characteristics or user physiological characteristics change. However, in running time, there is no automatic method to assess when the precision of the mapping model will decline and online compensation is difficult. Therefore, routine offline calibration is a necessary task (Gomez & Gellersen, 2018). At present, the

existing calibration methods come in two categories: calibration based on distributed static target points and smooth pursuit calibration. Calibration based on distributed static target points displays a set of specific static target points on the screen and requires the user to gaze at each of the target points for a period of time, one at a time (Harezlak, Kasprowski, & Stasch, 2014). This calibration method varies with different researchers in the number of target points, layout, length of time to gaze at the target point, and type of mapping algorithm. Theoretically, the more points there are, the higher the precision of the model estimation. However, the calibration process is usually characterized by tedious repetition, user fatigue and low ease of use (Drewes, Pfeuffer, & Alt, 2019). Therefore, researchers have proposed smooth pursuit calibration (Pfeuffer, Vidal, Turner, Bulling, & Gellersen, 2013), making use of the user's attention mechanism by naturally gazing at moving targets for calibration. The results show that compared with the distributed standard 9-point static calibration, not only does the smooth pursuit calibration cover a wider space and the calibration precision is improved but also the calibration time is shortened and the process is easy to use.

The smooth pursuit method has a unique advantage for people with difficulty in gaze fixation. In 2017, Pfeuffer (Pfeuffer et al., 2013) proposed completing the calibration task by using the smooth pursuit calibration method for people with difficulty concentrating (such as autistic children). The experimental results show that when the calibration target points move along the horizontal uniform path, the wave horizontal path and vertical path, the mean error can reach within 1°, which is better than the fixation error of 1.15° with 28 static points, but the whole calibration process takes 30 s to 60 s. In 2018, Argenis Ramirez Gomez (Gomez & Gellersen, 2018) et al. proposed a new smooth tracking calibration mechanism named smooth-i, which detects the motion area by motion matching and collects motion points to create a calibration profile. When the user tracks a moving target, the line of sight and the contour trajectory match, and data points are automatically collected. If there are inaccurate points, the modified mapping model is recalibrated. in 2019, Yasmeen (Abdrabou, Mostafa, Khamis, & Elmougy, 2019) et al. applied gaze estimation based on smooth pursuit to text input for disabled users as the speed and precision of smooth tracking and improved the average input rate. Most of the studies on smooth tracking calibration are online calibrations with moving targets during the use of eye tracking equipment. Although a separate offline calibration

step is omitted and the fixation error can also reach 1°, it does not apply if there is no moving target during the use of eye tracking equipment; therefore, a deliberate calibration with visual guidance has to be summoned from time to time.

In the strategy of fine calibration to reduce the fixation error, there are two main methods: calibration mode-based calibration and data-driven recalibration. The calibration mode-based approach reduces errors caused by system variables, focusing on calibration with choosing an appropriate layout of distributed static targets and a method of data integration. For example, Adithya(Adithya, Hanna, Kumar, & Chai, 2018) et al. used multiple sets of calibration points in initial calibration to reduce errors; Harrar (Harrar, Le Trung, Malienko, & Khan, 2018) et al. proposed using five groups of different types of calibration methods of distributed static target points and taking the average (directly watching the calibration point or closing to the invisible calibration point by prompt). The average value of the results is lower than the error caused by only one calibration method. The working principle of the data-driven calibration method is that the error is further eliminated by modeling residual error from the initial calibration data, which is also called secondary calibration or recalibration. Because they do not need to modify the existing calibration program or reconstruct the usual white-box mapping model of gaze estimation, it only needs to process the collected eye movement data by numerical methods. For example, Yunfeng Zhang (Zhang & Hornof, 2014) et al. proposed using an independent quadratic polynomial regression to estimate the error in the X and Y directions to compensate for the measurement results of the eye tracker. Argenis (Gomez & Gellersen, 2018) et al proposed using a quadratic polynomial as a calibration function by substituting the trajectory of the movement into the calibration function to calculate the error. If the error is greater than the set threshold, real-time recalibration can be taken to reduce the error. Zineb (Zineb, Rachid, & Talbi) et al. used thin plate splines (TPS) as a surrogate model for a surrogate-based optimization algorithm, which improved the speed and precision of calibrations.

We modeled the residual error by a data-driven method, considered the effect of the static distribution of target points on the data, and proposed a smooth pursuit calibration method based on the modulated guiding trajectory. This method made use of the data from the initial calibration of the eye tracking equipment. We established a calibration trajectory in the recalibration task and modulated its spatial-temporal characteristics to reduce the influence of error sources, thereby improving the calibration performance. Through systematic experiments, we found that the gaze point error of the smooth curve trajectory has a correlation with the velocity curve of the gaze trajectory. When the velocity exceeds a threshold (approximately 6°/s is found to be a critical point), the gaze error in the X and Y directions increases significantly with increasing velocity in both the X and Y directions. Based on these findings and considering the general characteristics of the spatial distribution of eye tracking error, the guidance trajectory was designed, and its speed was modulated within an appropriate range. The target calibration point moves according to the guidance trajectory, and gaze data are collected at the same time. Without changing the underlying physical mapping model of eye movement tracking equipment, a gaze error compensation model was established through neural network learning. The experimental results have shown that the mean error of the user gaze point estimation decreases to approximately 0.4° from the initial value of approximately 1.0°, and the time spent in the whole calibration process is approximately 45 s, which has the advantages of being easy to use, fast and precise.

2 METHODS

2.1 Smooth Pursuit with Regulated Visual Guidance and Tracking Data Collection for Recalibration

The moving target point of the smooth pursuit calibration program is composed of a circle with a diameter of 20 pix and a center diameter of 10 pix. The initial position is located at the center of the blue calibration plane of the interface, as shown in Figure 2. The calibration gaze point (the green point) follows the spatial trajectory with certain temporal characteristics. In our previous experiments, two calibration modes of hidden and visible smooth calibration curve trajectories in the calibration window were tested. It was found that the two collection methods had little influence on data quality.

In the following experiment in this work, the calibration window was configured to show the calibration trajectory while collecting data. According to the motion of the calibration points, a large number of target points can be extracted from the continuous gaze data. In the calibration window

of 1600x900 pixels, the calibration data collection process takes approximately 35 s. According to the condition that the time stamp of the target point is no more than 5 ms ahead of the time stamp of the eye tracking data, no less than 2000 groups of target point data can be collected on the trajectory. According to the conclusions drawn by Harezlak (Harezlak et al., 2014) et al. and our multiple experimental analysis, the eye movement data are unreliable within the first 600 ms to 700 ms when the smooth pursuit calibration starts to collect gaze data. Therefore, in the calibration process proposed, the target point will jump 750 ms in situ after clicking the calibration start button, which is mainly based on two considerations: 1. To avoid collecting unreliable data; 2. To remind users that the smooth pursuit calibration program is about to start, they need to pay attention at this time.

Considering the border-oriented trend of the error distribution characteristics of the eye tracking system, as shown in Figure 1, and its relative stability for specific equipment, initial calibration configuration and individual experimental personnel, the appropriate trajectory can be roughly determined by the error spatial distribution before fine recalibration. The spatial guidance trajectory design example with an uneven density distribution is shown in Figure 2. As shown there, the pursuit calibration trajectory is segmentally smooth with the higher line density where the closer to boarder.
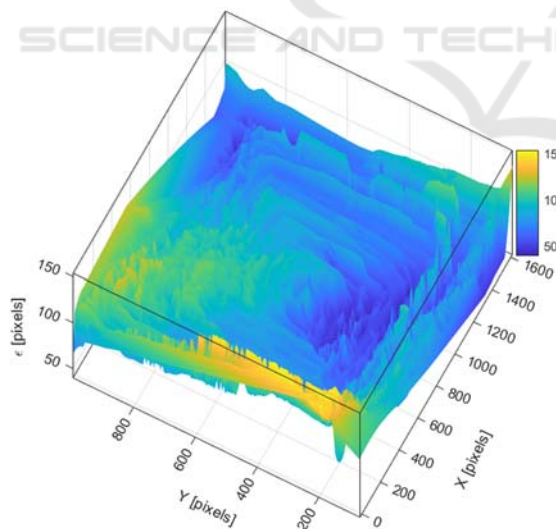

Figure 1: Typical spatial distribution of gaze error (where X and Y are gaze coordinates along horizontal and vertical directions; ε is gaze error defined by Euclidean distance).

In addition, the time modulation of the guidance trajectory needs to be considered. Considering the physiological characteristics of human visual

tracking, it is conjectured that motion speed is an important factor affecting trajectory calibration error. The repeated linear path with different uniform velocities and curve paths with varying velocities are designed in prelude experiments to verify the correlation between speed and tracking error and to determine the appropriate speed threshold, which provides the basis for the calibration trajectory regulation. On the other hand, the repeatability precision analysis of the tracking data in prelude experiments also provides evidence for the potentiality of improving accuracy.

Figure 2: Spatially nonuniform square spiral trace on the X-Y plane with limited speed designed for model learning.

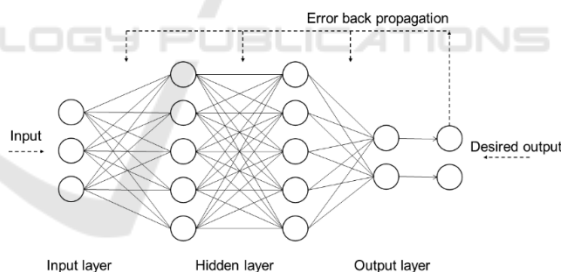## 2.2 Recalibration Model for Regulated Smooth Pursuit

Figure 3: Structural diagram of the BP neural network.

The data-driven recalibration method is widely used. The error model is learned from the data, and the error characteristics are extracted to reduce the error. A large number of researchers (Blignaut, Holmqvist, Nyström, & Dewhurst, 2014; Drewes et al., 2019; Huang, Kwok, Ngai, Chan, & Leong, 2016; Zhang & Hornof, 2014) established the recalibration model through the regression method. The regression method is simple, and the program execution is fast. Simple linear regression and low-order polynomial regression cannot obtain a good fit. The BP neural network (Rumelhart, Hinton, & Williams, 1986) is a network model based on error backpropagation. As shown in Figure 3, the BP network contains an input

layer, output layer, and one or more hidden layers. There is no feedback path across layers and no interconnection within each layer. All neurons are connected between adjacent layers. Although it has a simple structure, it can learn a large number of input and output mapping relationships with high efficiency, taking less than 10 s with more than 2000 data points in our case. The experimental results of Harezlak (Harezlak et al., 2014) et al. also show that artificial neural networks have a good error calibration capability.

3 EXPERIMENTS

3.1 Equipment

In this study, we use the Tobii 4c eye tracking system, which is based on the PCCR principle (as shown in Figure 4), with a recommended working distance of 50 ~ 95 cm and a near infrared (NIR 850 nm) light source. The calculation equipment is a Dell XPS8940 PC, Windows 10 64-bit OS, 3.5 GHz Intel i9 CPU. The eye tracking equipment is installed under a 28-inch Samsung monitor with a resolution of 3840x2160. All data samples are streamed at 60 Hz from the Tobii official driver with an initial calibration, which is done once and indefinitely.
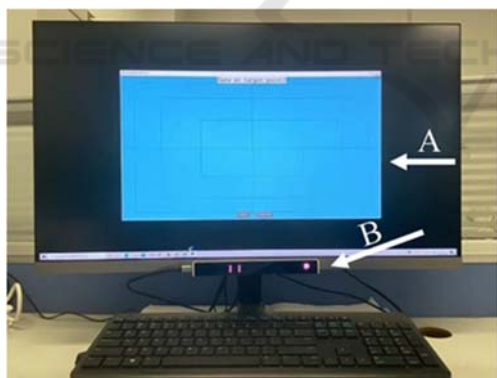

Figure 4: Working environment of eye tracking equipment (A refers to the calibration window; B refers to the eye tracking equipment).

3.2 Procedure and Results

During the experiment, to verify the influence of the speed of the target gaze point on the tracking error, we repeated the measurement and collected the eye movement fixation data for analysis. The eye fixation data were measured by the movement of the eyeball following the target point along the horizontal line and the vertical line. Seven groups of experiments

were performed at speeds of 2, 4, 6, 8, 10, 12 and 14 °/s. Each group of experiments was repeated ten times. Figure 5 shows the spatial traces and absolute error distribution of measured gaze points of all groups/repetitions with eyeballs following the target points along the horizontal straight trajectory. Similar to the vertical straight-line trajectory, Figure 6 shows the spatial traces and absolute error distribution of the measured gaze points of all groups/repetitions with eyeballs following the moving target fixation point.

It can be observed from the error distribution in Figures 5 and 6 that the eye gaze error of smooth tracking under multiple repeated measurements is not random, and with the increase of the gaze moving speed in each axis, the absolute error gradually increases, and the dispersion degree of distribution also increases. However, it can be seen that when the gaze velocities in the X and Y directions are both within 6°/s, the direction errors are not prominently differentiable between each group and tend to be stable within each group. To further verify the effect of gaze movement speed on gaze error, we conducted an experiment of variable-speed gaze movement in the Y direction. We set three groups of gaze movement trajectories with large variance, and each group repeated five times. The target guided the gaze point to move at a constant speed in the horizontal direction and at a variable speed in the vertical direction. The spatial traces, vertical velocity distribution and vertical error distribution (nonabsolute value) of the measured gaze points of all groups/repetitions with eyes following the movement of the target gaze point are shown in Figure 7.

From the data distribution of Figure 7, we can further observe that there is an obvious correlation between the velocity curve and the error curve in the corresponding axis. When the velocity curve reaches the extreme value, the direction error also reaches the extreme value in the corresponding section with slight phase shifting.

Combined with the characteristics of Figure 5, Figure 6 and Figure 7, we set the moving speed of the calibration fixation point to 5.4°/s (equivalent to 2 pix/s for the experimental device) to follow the target calibration trajectory, and the data generated are used to train the neural network. However, five velocity modulation trajectories with large variances are randomly generated with the fixation point moving at a constant velocity in the X direction and at a velocity modulated to less than 6°/s in the Y direction to predict and verify the error compensation model.

Table 1 shows the error table of fixation data collected by an experimenter based on the Tobii 4c
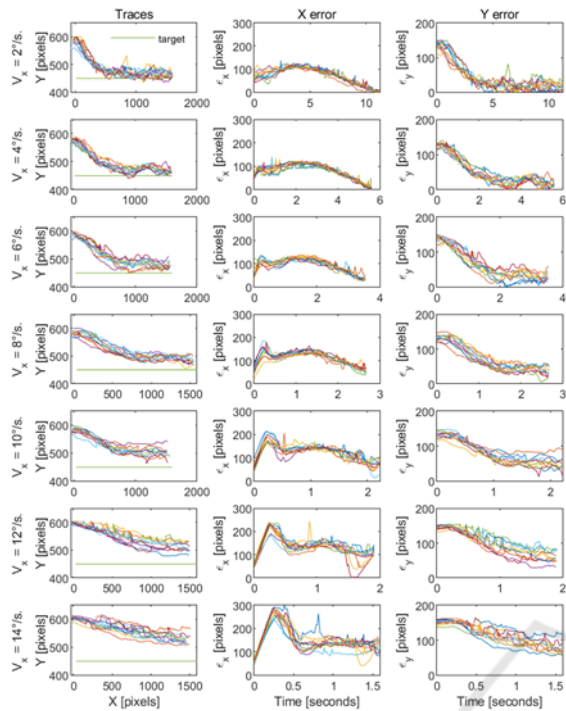
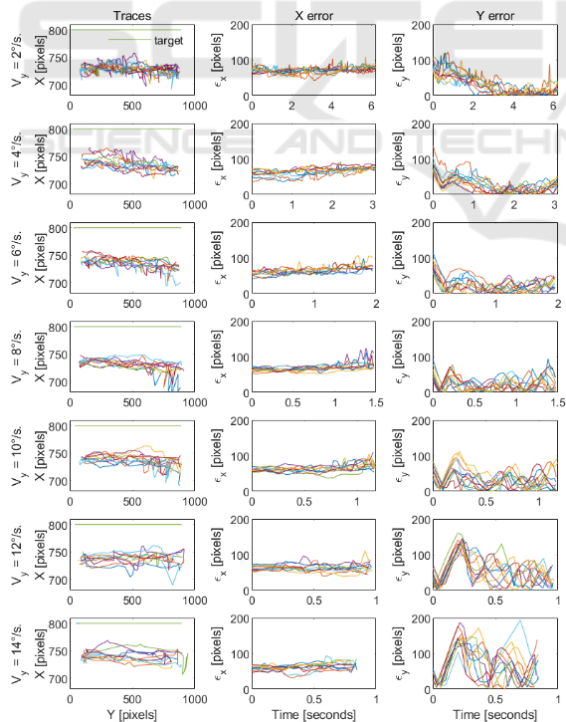Figure 5: Horizontal line tracking with different constant X velocities.

Figure 6: Vertical line tracking with different constant Y velocities (note X and Y swapped in the 'Traces' column).
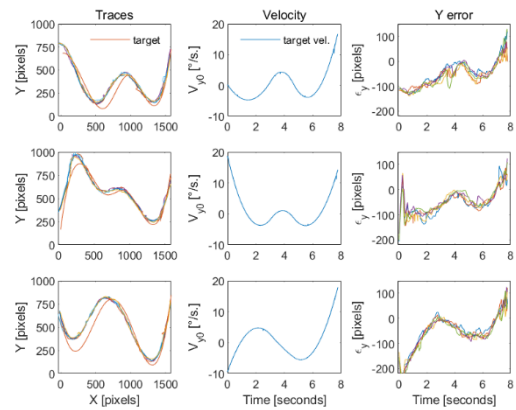

Figure 7: Tracking error with limited varying Y velocities.

Table 1: Multiple sets of gaze point dataset error (a. Errors in degrees as unit; b. Errors in pixels. In the figures, Trace_calibration data are used for calibration, Trace_1~5 are used for testing the recalibration model later, as shown in Table 2, and X_mae and Y_mae are the mean absolute errors in the horizontal and vertical directions, respectively).

Error（degrees）			
Test (experiments number）	X_mae	Y_mae	mae
Trace_calibration	0.81	0.70	1.07
Trace_1	0.69	0.81	1.06
Trace_2	0.84	0.74	1.12
Trace_3	0.80	0.80	1.13
Trace_4	0.72	0.61	0.94
Trace_5	0.73	0.61	1.13

(a)

Error（pixels）			
Test (experiments number）	X_mae	Y_mae	mae
Trace_calibration	59	51	78
Trace_1	50	59	77
Trace_2	61	54	81
Trace_3	58	59	83
Trace_4	53	45	70
Trace_5	54	45	70

(b)

fixation smoothing calibration trajectory and five randomly generated test trajectories (before the recalibration model is applied), including the average absolute error and the maximum absolute error in the X direction and the average absolute error and the maximum absolute error in the Y direction. In the process of eye movement data collection, the measurement process of eye movement is independent and parallel with the movement of the target fixation point without interfering with each other. Finally, according to their respective timestamps, the advantages of independent and

parallel visualizing and sampling are to ensure the real-time performance of measurement data to the greatest extent, preventing the inaccurate measurement caused by the time fluctuation noise. The collected data include the position and time stamp of the target point on the screen (x_target, y_target, unit: pix; timestamp, unit: us), Tobii 4c measurement data and timestamp (timestamp, unit: us), tobii 4c measurement data include the measurement of user's eye fixation on the screen and data validity flag (x_meas, y_meas, unit: pix; validity, as 0 or 1), the spatial location of the user's left eye relative to the center of the screen, and the data validity signs (x_lefteye, y_lefteye, z_lefteye, unit: mm; valid, as 0 or 1), the spatial location of the user's right eye relative to the center of the screen (x_righteye, y_righteye, z_righteye, unit: mm; validity, as 0 or 1). Before training the BP neural network model, it is necessary to filter the data whose filtering time difference is greater than the predefined threshold (set to 5 ms) or validty = 0. With validity = 0, it indicates that the sampling data of eye movement equipment are invalid, which situation will occur if at the sampling moment eyes are closed or the user is not in the working space of the eye movement tracking equipment.

Table 2: Corrected fixation data against Table 1 (a. Errors in degrees as units; b. Errors in pixels. Trace_1~5 data are used again to test the recalibration model trained by Trace_calibration data, as shown in Table 1. X_mae and Y_mae are the mean absolute errors after correction in the horizontal and vertical directions, respectively).

Error(degrees)				
Test (experiments number)	X_mae	Y_mae	mae	R2_score
Trace_1	0.22	0.21	0.30	0.989
Trace_2	0.30	0.22	0.37	0.995
Trace_3	0.25	0.29	0.38	0.987
Trace_4	0.30	0.17	0.34	0.996
Trace_5	0.23	0.26	0.35	0.990

(a)

Error (pixels)			
Test (experiments number)	X_mae	Y_mae	mae
Trace_1	16	16	23
Trace_2	22	16	27
Trace_3	19	21	28
Trace_4	22	13	26
Trace_5	17	19	25

(b)

An appropriate mapping model is established based on the machine learning library Sklearn and BP neural network structure. The calibration dataset

collected in a group of experiments by an experimenter is used for training by using the appropriate model structure and method, determining the appropriate hidden layer number and node number, selecting ReLU (f(x) = max(0, x)) as the activation function, Adam as the optimization method, x_meas, y_meas, x_lefteye, y_lefteye, z_lefteye, x_righteye, y_righteye, z_righteye as the feature input, and x_target, y_target as the output.

We train Trace_calibration (calibration dataset) based on the BP neural network and test the Trace_1 to Trace_5 fixation datasets based on the obtained training model. The results are shown in Table 2.

In Table 2, R2_score (Raju, Bilgic, Edwards, & Fleer, 1997; Yin & Fan, 2001) is a kind of model accuracy evaluation index with $R2_{score} = 1 - \frac{\sum_i(\hat{y}^{(i)} - y^{(i)})^2}{\sum_i(\bar{y}^{(i)} - y^{(i)})^2}$, where i is the time point index in a single test trace, y is the target gaze point, $\hat{y}$ is the model corrected prediction from gaze measurement, and $\bar{y}$ is the temporal average of y. Figure 8 shows the corresponding visualization of these model-based recalibration results (with error in pixels) tested by the random curve trajectory fixation datasets (Trace_1 to Trace_5).
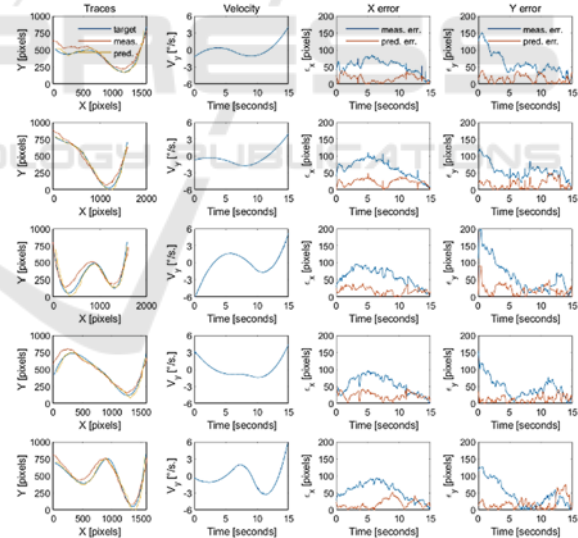

Figure 8: Spatially randomly generated curves tracking with temporally limited speed for model verification.

4 DISCUSSION

In this study, a smooth pursuit calibration method based on velocity modulation was proposed, and the correction effect of the BP neural network model on

the eye movement data generated randomly but satisfying the regulation was verified.

Before recalibration, the mean absolute error of the fixation point was approximately 1.0°. After several experimental measurements of the smooth calibration trajectory, the data trajectory of the fixation point measured by the eye tracking equipment basically features small variance, which can also be seen from Figures 5 and 6. This mainly reflects the high repeatability performance of the eye tracking equipment, and there is statistical regularity underpinning the residual error with high confidence. There is a potentiality that the error can be effectively reduced through an appropriate recalibration model.

Meanwhile, we found that there is a correlation between the error curve of the fixation point and the velocity curve in the varying velocity experiment. We carried out seven groups of uniform motion tracking experiments of horizontal and vertical lines, with speeds set as 2, 4, 6, 8, 10, 12, and 14°/s, respectively, and found that when the velocity of the fixation point exceeds 6°/s, the error gradually diverges, and the error curve becomes much more uncertain. Therefore, in the formal experiment of smooth pursuit for calibration, the speed of the target gaze point should be kept smaller than 6°/s.

In our calibration experiment, we assume that the BP neural network can predict the uncollected gaze data points by learning the data from the calibration curve to effectively reduce the residual error. This assumption is indeed verified. We found that the randomly generated test curve showed an obvious decrease in error when applying the learnt model, with the adjustment of the appropriate training parameters (nonlinearity). In addition, the regression model of the number of layers and nodes of the BP neural network is established quickly with a good error compensation effect. The average absolute error of the smoothing calibration based on visual guidance is lowered to approximately 0.4° from 1.0° within 10 s to finish training.

In addition, the experimenters may feel dry and uncomfortable in the eyes in the process of calibration procedures; if they deliberately avoid blinking, this is the manifestation of extraocular eye muscle fatigue (Sun, 2003). This situation will make the fixation data change greatly in a short period of time. From the original error curve in Figure 5 and Figure 6, it can be observed that there are some erroneous jittering points, which is the blinking situation described. The occasional error jitters will not affect the calibration effect of the model. In the calibration process, it is just enough to relax and focus, and it is not necessary to deliberately keep eyes open because extraocular eye

muscles are not fatigable in normal usage, similar to jaw muscles (Fuchs & Binder, 1983).

5 CONCLUSION AND FUTURE WORK

In previous research on smooth pursuit calibration, it is generally necessary for users to gaze at the moving target during the normal use of eye tracking equipment and recalibrate with the target location in running time. Although this smooth calibration method eliminates the calibration steps before the formal use of eye movement tracking equipment, it does not work well without a moving target in the use process. In our study, we found a correlation between speed and tracking error through experiments and proposed smooth pursuit calibration with speed-modulated visual guidance to collect the appropriate gaze data. We found the appropriate method to establish the data calibration model. The sampling and training of the recalibration process is fast, within 45s to complete, and the gaze point has a significantly smaller error than the official calibration. In the course of our experiment, it is found that displaying the smooth calibration curve in the calibration window can make users focus more naturally and avoid visual fatigue.

In future research, we will study the influence of the history and the future trajectory of the smooth calibration curve near the current target point on the model performance and design a learning algorithm to replace the function of the smooth trajectory visual guidance so that it is more suitable for a more general and practical working scenario.

ACKNOWLEDGMENTS

REFERENCES

Abdrabou, Y., Mostafa, M., Khamis, M., & Elmougy, A. (2019, June). Calibration-free text entry using smooth pursuit eye movements. In *Proceedings of the 11th ACM Symposium on Eye Tracking Research & Applications* (pp. 1-5).

Adithya, B., Hanna, L., Kumar, P., & Chai, Y. J. T. (2018). Calibration techniques and gaze accuracy estimation in pupil labs eye tracker. *TECHART: Journal of Arts and Imaging Science*, *5*(1), 38-41.

Blignaut, P., Holmqvist, K., Nyström, M., & Dewhurst, R. (2014). Improving the accuracy of video-based eye tracking in real time through post-calibration regression. In *Current Trends in Eye Tracking Research* (pp. 77-100)

Drewes, H., Pfeuffer, K., & Alt, F. (2019, June). Time-and space-efficient eye tracker calibration. In *Proceedings of the 11th ACM Symposium on Eye Tracking Research & Applications* (pp. 1-8)

Gomez, A. R., & Gellersen, H. (2018, June). Smooth-i: smart re-calibration using smooth pursuit eye movements. In *Proceedings of the 2018 ACM Symposium on Eye Tracking Research & Applications* (pp. 1-5).

Guestrin, E. D., & Eizenman, M. (2006). General theory of remote gaze estimation using the pupil center and corneal reflections. *IEEE Transactions on biomedical engineering*, *53*(6), 1124-1133.

Hansen, D. W., & Ji, Q. (2009). In the eye of the beholder: A survey of models for eyes and gaze. *IEEE transactions on pattern analysis and machine intelligence*, *32*(3), 478-500.

Harezlak, K., Kasprowski, P., & Stasch, M. (2014). Towards accurate eye tracker calibration–methods and procedures. *Procedia Computer Science*, *35*, 1073-1081.

Harrar, V., Le Trung, W., Malienko, A., & Khan, A. Z. (2018). A nonvisual eye tracker calibration method for video-based tracking. *Journal of Vision*, *18*(9), 13-13.

Holmqvist, K., Nyström, M., Andersson, R., Dewhurst, R., Jarodzka, H., & Van de Weijer, J. (2011). *Eye tracking: A comprehensive guide to methods and measures*. OUP Oxford.

Huang, M. X., Kwok, T. C., Ngai, G., Chan, S. C., & Leong, H. V. (2016, May). Building a personalized, auto-calibrating eye tracker from user interactions. In *Proceedings of the 2016 CHI Conference on Human Factors in Computing Systems* (pp. 5169-5179).

Larrazabal, A. J., Cena, C. G., & Martínez, C. E. (2019). Video-oculography eye tracking towards clinical applications: A review. *Computers in biology and medicine*, *108*, 57-66.

Mahmud, S., Lin, X., & Kim, J. H. (2020, January). Interface for Human Machine Interaction for assistant devices: a review. In *2020 10th Annual Computing and Communication Workshop and Conference (CCWC)* (pp. 0768-0773).

Zineb, T., Rachid, E., & Talbi, E. G. (2019, October). Thin-plate spline RBF surrogate model for global optimization algorithms. *In 2019 1st International Conference on Smart Systems and Data Science (ICSSD)* (pp. 1-6).

Pfeuffer, K., Vidal, M., Turner, J., Bulling, A., & Gellersen, H. (2013). Pursuit calibration: Making gaze calibration less tedious and more flexible. In *Proceedings of the 26th annual ACM symposium on User interface software and technology* (pp. 261-270).

Raju, N. S., Bilgic, R., Edwards, J. E., & Fleer, P. F. (1997). Methodology review: Estimation of population validity and cross-validity, and the use of equal weights in prediction. *Applied Psychological Measurement*, *21*(4), 291-305.

Rumelhart, D. E., Hinton, G. E., & Williams, R. J. (1986). Learning representations by back-propagating errors. *nature*, *323*(6088), 533-536.

Valtakari, N. V., Hooge, I. T., Viktorsson, C., Nyström, P., Falck-Ytter, T., & Hessels, R. S. (2021). Eye tracking in human interaction: Possibilities and limitations. *Behavior Research Methods*, *53*(4), 1592-1608.

Yin, P., & Fan, X. (2001). Estimating R 2 shrinkage in multiple regression: A comparison of different analytical methods. *The Journal of Experimental Education*, *69*(2), 203-224.

Zhang, Y., & Hornof, A. J. (2014, March). Easy post-hoc spatial recalibration of eye tracking data. In *Proceedings of the symposium on eye tracking research and applications* (pp. 95-98).

Zhu, Z., & Ji, Q. (2005, June). Eye gaze tracking under natural head movements. In *2005 IEEE Computer Society Conference on Computer Vision and Pattern Recognition (CVPR'05)* (Vol. 1, pp. 918-923).

Sun, H. B. (2003), Why do we blink? *Journal of biology teaching* (in Chinese), 2003(12), 52-52.

Fuchs, A. F., & Binder, M. D. (1983). Fatigue resistance of human extraocular muscles. *Journal of neurophysiology*, *49*(1), 28-34.